American Mineralogist, Volume 64, pages 1248–1254, 1979

Krautite, $Mn(H_2O)(AsO_3OH)$: crystal structure, hydrogen bonding and relations with haidingerite and pharmacolite

MICHELE CATTI AND MARINELLA FRANCHINI-ANGELA

Istituto di Mineralogia, Cristallografia e Geochimica "G. Spezia"
Università di Torino, Via S. Massimo 22, 10123 Torino, Italy

Abstract

The crystal structure of synthetic krautite was solved (direct methods) and refined isotropically ($R = 0.112$) in space group $P2_1$ with 2294 reflections measured on a single-crystal diffractometer, with Mo$K\alpha$ radiation. The unit-cell parameters are: $a = 8.012(2)$, $b = 15.956(4)$, $c = 6.801(2)A$, $\beta = 96.60(3)°$; $Z = 8$. A strong $P2_1/n$ pseudosymmetry appears in the structure, yet the average pseudo-center is slightly shifted from the correct position 1/4, 0, 1/4 in space group $P2_1/n$. The structure is built up by (010) layers of AsO_4 and MnO_6 coordination polyhedra. In each layer, MnO_6 octahedra share edges to form $[10\bar{1}]$ chains, which sandwich the AsO_4 tetrahedra. Adjacent layers are related by the screw axis and are linked by four out of twelve independent hydrogen bonds; two of them are acidic and two are donated by water molecules. One of the latter hydrogen bonds is probably bifurcated, since the water molecule is involved in two contacts 2.92 and 3.08A long. Haidingerite ($CaHAsO_4 \cdot H_2O$) and pharmacolite ($CaHAsO_4 \cdot 2H_2O$) show similar structures formed by layers of coordination polyhedra connected by hydrogen bonds. For the single-layer topology, krautite resembles pharmacolite (chain-like structure) more than haidingerite (network-like structure), since the increase of coordination number from Mn^{2+} to Ca^{2+} is compensated by the increase of water content.

Introduction

In a series of structural and crystal-chemical investigations on mineral arsenates containing hydrogen bonds (Catti *et al.*, 1977), the manganese arsenate krautite, recently described and characterized as a new mineral by Fontan *et al.* (1975), has been examined. The other known natural manganese arsenates are a large group of basic arsenates (Moore, 1967), manganese hoernesite $(Mn, Mg)_3(AsO_4)_2 \cdot 8H_2O$, and the new mineral $CaMn(HAsO_4)_2 \cdot 2H_2O$ (Permingeat *et al.*, in preparation). The synthetic crystalline phases reported in the system $MnO–As_2O_5–H_2O$ (Pascal, 1966, p. 923) are $Mn_3(AsO_4)_2 \cdot H_2O$, $MnHAsO_4 \cdot H_2O$, $Mn(H_2AsO_4)_2$, $Mn(H_2AsO_4)_2 \cdot 3H_2O$, and $MnHAsO_4 \cdot 4H_2O$; the last compound is probably isomorphous with brassite, $MgHAsO_4 \cdot 4H_2O$, the structure of which is known (Protas and Gindt, 1976). Krautite is the first acid manganous arsenate studied structurally; we aim to clarify the crystal-chemical relationships with its calcium homolog haidingerite, $CaHAsO_4 \cdot H_2O$ (Cassien *et al.*, 1966; Calleri and Ferraris, 1967). Indeed, both minerals show very similar cell parameters and strong mica-like (010) cleavages, so that analogous layered structure types seem appropriate, in spite of the fact that the symmetries are different (monoclinic for krautite and orthorhombic for haidingerite), and important differences appear in their X-ray powder patterns.

Experimental

Since good quality single crystals could not be found in the natural samples of krautite (Fontan *et al.*, 1975), synthetic crystalline $MnHAsO_4 \cdot H_2O$ was prepared. By mixing aqueous solutions of $MnCl_2$ and KH_2AsO_4 a transparent gel was obtained (Deiss, 1914), from which many small pink balls (about 2 mm diameter) precipitated; each ball was formed by tiny, crystalline packets of $MnHAsO_4 \cdot H_2O$. Every packet contained very thin {010} lamellae, with frequent polysynthetic twinning. With great difficulty an irregular crystalline fragment $0.30 \times 0.10 \times 0.02$ mm could be isolated, and was used for all measurements.

By means of Weissenberg photographs and single-crystal diffractometry the monoclinic unit cell

0003–004X/79/1112–1248$02.00

reported by Fontan *et al.* was confirmed. The least-squares refinement of 25 θ values measured on a diffractometer [λ(Mo$K\alpha$) = 0.71069A] yielded the unit-cell parameters a = 8.012(2), b = 15.956(4), c = 6.801(2)A, β = 96.60(3)°. Other crystal data are: V = 863.7A^3, Z = 8, M = 212.879, ρ (meas) = 3.30 g cm^{-3} (Fontan *et al.*, 1975), ρ (calc) = 3.274 g cm^{-3}, F(000) = 1128, μ(Mo$K\alpha$) = 111.7 cm^{-1}. On the basis of systematic absences, the space group could be either $P2_1$ or $P2_1/m$; an analysis of statistical tests on the diffraction intensities to detect the symmetry center gave ambiguous results.

The intensities were measured on a Philips PW 1100 automatic four-circle diffractometer with the following conditions: Mo$K\alpha$ radiation, graphite monochromator, $\theta \leq 30°$, ω scan, $\Delta\omega$ = 1.40°, scanning speed 0.04° s^{-1}, background time 5 sec on both sides of each peak, attenuating filter inserted for intensities higher than 60000 counts s^{-1}, three reference reflections. By removing the reflections with $|F_o| \leq 3\sigma(|F_o|)$, 2294 independent observations remained for this study.[1]

Solution and refinement of the structure

The program MULTAN based on direct methods (Germain *et al.*, 1971) was used to solve the structure. In the centrosymmetrical space group $P2_1/m$ only pseudo-solutions were obtained; the correct solution was found in the non-centrosymmetrical space group $P2_1$, showing the positions of the four As and four Mn independent atoms. By subsequent structure-factor calculations and Fourier difference maps, all the oxygen atoms were located. The full-matrix least-squares refinement with isotropic temperature factors for all atoms converged to R = 0.112; anomalous scattering of As and Mn atoms was corrected for, and the y coordinate of As(1)[2] was locked during the refinement to fix the origin. The following weighting scheme was used: $w = 1/(5 \times 10^{-4}|F_o|^2 + 1)$; then the average values of Δ^2 for groups of reflections were practically constant. An anisotropic refinement was tried unsuccessfully, since the temperature factors of several atoms became non-positive–definite. No absorption correction could be performed, owing to the irregularity of the crystalline fragment; this must have introduced large systematic errors into the data, because of the lamellar shape of the crystal and of the large value of the linear absorption coefficient, and would account for the failure of the anisotropic refinement. Table 1 reports the final atomic fractional coordinates; large values of the *e.s.d.*'s can be observed and could be ascribed to the pseudo-symmetry of the structure (*cf.* the discussion), which causes a high correlation between atomic positional parameters in the refinement.

Table 1. Atomic fractional coordinates and thermal parameters (A^2)

	x	y	z	B
Mn(1)	0.4033(4)*	0.0451(2)	0.6520(4)	0.69(4)
Mn(1')	0.1069(4)	-0.0455(2)	0.9043(4)	0.76(4)
Mn(2)	0.8581(4)	0.0663(2)	0.1631(4)	0.71(4)
Mn(2')	0.6511(4)	-0.0661(2)	0.3934(4)	0.70(4)
As(1)	0.4087(2)	0.0874(1)	0.1473(3)	0.61(3)
As(1')	0.1000(2)	-0.0881(1)	0.4075(3)	0.57(3)
As(2)	0.8140(2)	0.1014(1)	0.6689(3)	0.52(3)
As(2')	0.6976(2)	-0.1035(1)	0.8891(3)	0.52(3)
O(1)	0.297(2)	0.171(1)	0.202(2)	1.1(2)
O(1')	0.211(2)	-0.169(1)	0.351(2)	1.1(2)
O(2)	0.329(2)	0.036(1)	-0.054(2)	0.7(2)
O(2')	0.183(2)	-0.036(1)	0.612(2)	1.0(2)
O(3)	0.449(2)	0.023(1)	0.342(2)	0.9(2)
O(3')	0.058(1)	-0.022(1)	0.214(2)	0.3(2)
O(4)	0.603(2)	0.129(1)	0.092(2)	1.3(2)
O(4')	-0.090(2)	-0.129(1)	0.462(2)	0.7(2)
O(5)	0.624(2)	0.134(1)	0.717(2)	1.1(2)
O(5')	0.888(2)	-0.133(1)	0.841(2)	0.7(2)
O(6)	0.916(2)	0.050(1)	0.862(2)	0.7(2)
O(6')	0.593(2)	-0.051(1)	0.696(2)	0.9(2)
O(7)	0.808(2)	0.044(1)	0.462(2)	1.0(2)
O(7')	0.707(2)	-0.045(1)	1.097(2)	0.9(2)
O(8)	0.938(2)	0.189(1)	0.644(2)	1.4(2)
O(8')	0.583(2)	-0.190(1)	0.922(3)	1.6(3)
W(1)	0.264(2)	0.164(1)	0.583(2)	1.5(2)
W(1')	0.248(2)	-0.166(1)	0.964(2)	1.4(2)
W(2)	0.960(2)	0.190(1)	0.168(3)	1.8(3)
W(2')	0.545(2)	-0.187(1)	0.391(3)	1.8(3)

* Estimated standard deviations are given in parentheses and refer to the last decimal place.

Discussion

Pseudo-symmetry and description of the structure

A strong $P2_1/n$ pseudo-symmetry is shown by inspection of Table 1. All atoms can be grouped in pairs related by a pseudo-center of inversion, which is located on the average at x = 0.2555, y = 0, z =

[1] To receive a copy of the structure factor table, order Document AM-79-113 from the Business Office, Mineralogical Society of America, 2000 Florida Avenue, NW, Washington, D. C. 20009. Please remit $1.00 in advance for the microfiche.

[2] A single figure in parentheses denotes an atom of the asymmetric unit; primed figures mean the pseudo-symmetry operation 1/2 − x, $\bar{y}$, 1/2 − z. The second figure 2 is included for atoms in the equivalent position $\bar{x}$, 1/2 + y, $\bar{z}$. Roman numerals represent the following translations: I, −**c**; II, +**c**; III, −**a**; IV, +**a**; V, +**a** − **b** + **c**; VI, +**a** + **c**; VII, +2**a** + **c**.

Table 2. Interatomic distances and O–As–O angles in the four independent AsO_4 groups

As(1) – O(1)	1.67(2)*	Å	As(1') – O(1')	1.64(2)	Å
As(1) – O(2)	1.65(1)		As(1') – O(2')	1.69(1)	
As(1) – O(3)	1.67(1)		As(1') – O(3')	1.69(1)	
As(1) – O(4)	1.77(2)		As(1') – O(4')	1.73(1)	
Average	1.69		Average	1.69	
As(2) – O(5)	1.68(2)		As(2') – O(5')	1.66(1)	
As(2) – O(6)	1.68(1)		As(2') – O(6')	1.70(1)	
As(2) – O(7)	1.68(2)		As(2') – O(7')	1.69(1)	
As(2) – O(8)	1.73(2)		As(2') – O(8')	1.69(2)	
Average	1.69		Average	1.69	
O(1)...O(2)	2.79 Å	114.3°	O(1')...O(2')	2.79 Å	114.0°
O(1)...O(3)	2.76	111.6	O(1')...O(3')	2.76	111.8
O(1)...O(4)	2.73	104.9	O(1')...O(4')	2.69	105.5
O(2)...O(3)	2.76	111.9	O(2')...O(3')	2.78	111.1
O(2)...O(4)	2.74	105.9	O(2')...O(4')	2.74	106.4
O(3)...O(4)	2.78	107.6	O(3')...O(4')	2.76	107.5
Average	2.76		Average	2.75	
O(5)...O(6)	2.78 Å	111.9°	O(5')...O(6')	2.78 Å	111.6°
O(5)...O(7)	2.80	113.4	O(5')...O(7')	2.77	111.5
O(5)...O(8)	2.76	107.9	O(5')...O(8')	2.73	108.8
O(6)...O(7)	2.76	110.7	O(6')...O(7')	2.78	110.1
O(6)...O(8)	2.68	103.7	O(6')...O(8')	2.71	106.2
O(7)...O(8)	2.77	108.8	O(7')...O(8')	2.74	108.4
Average	2.76		Average	2.75	

* Estimated standard deviations for As–O distances are given in parentheses and refer to the last decimal place. The e.s.d.'s for O...O distances and for the angles are 0.02 Å and 0.7°, respectively.

Table 3. Interatomic distances and O–Mn–O angles in the Mn coordination polyhedra

Mn(1) – $O(2)^{II}$	2.16(1)*	Å	Mn(1') – O(2')	2.15(1)	Å
Mn(1) – O(3)	2.21(1)		Mn(1') – $O(3')^{II}$	2.22(1)	
Mn(1) – O(2')	2.18(1)		Mn(1') – $O(2)^{II}$	2.20(1)	
Mn(1) – O(5)	2.28(2)		Mn(1') – $O(5')^{III}$	2.24(1)	
Mn(1) – O(6')	2.15(1)		Mn(1') – $O(6)^{III}$	2.16(1)	
Mn(1) – W(1)	2.22(2)		Mn(1') – W(1')	2.24(2)	
Average	2.20		Average	2.20	
Mn(2) – O(4)	2.27(2)		Mn(2') – $O(4')^{IV}$	2.30(1)	
Mn(2) – $O(3')^{IV}$	2.13(1)		Mn(2') – O(3)	2.16(1)	
Mn(2) – $O(6)^{I}$	2.17(1)		Mn(2') – O(6')	2.17(1)	
Mn(2) – O(7)	2.15(2)		Mn(2') – $O(7')^{I}$	2.14(1)	
Mn(2) – $O(7')^{I}$	2.16(1)		Mn(2') – O(7)	2.18(2)	
Mn(2) – W(2)	2.13(2)		Mn(2') – W(2')	2.11(2)	
Average	2.17		Average	2.18	
$O(2)^{II}$...O(2')	2.70(2)*	Å 76.8°	O(2')...$O(2)^{II}$	2.70(2)	Å 76.6°
$O(2)^{II}$...O(5)	3.37(2)	98.8	O(2')...$O(5')^{III}$	3.35(2)	99.4
$O(2)^{II}$...O(6')	3.18(2)	95.2	O(2')...$O(6)^{III}$	3.20(2)	95.8
$O(2)^{II}$...W(1)	3.20(3)	93.9	O(2')...W(1')	3.16(3)	92.0
O(3) ...O(2')	3.11(2)	90.4	O(3')...$O(2)^{II}$	3.13(2)	90.2
O(3) ...O(5)	3.28(3)	94.2	O(3')...$O(5')^{III}$	3.26(2)	94.0
O(3) ...O(6')	2.81(2)	80.2	O(3')...$O(6)^{III}$	2.78(2)	79.0
O(3) ...W(1)	3.23(3)	93.8	O(3')...W(1')	3.32(2)	96.5
O(2')...O(6')	3.27(3)	98.1	O(2) ...$O(6)^{III}$	3.30(2)	98.6
O(2')...W(1)	3.27(3)	95.9	O(2) ...W(1')	3.29(3)	95.8
O(5) ...O(6')	2.97(3)	84.2	O(5')...$O(6)^{III}$	2.92(2)	83.4
O(5) ...W(1)	2.96(3)	82.3	O(5')...W(1')	2.95(3)	82.6
Average	3.11		Average	3.11	
O(4) ...$O(6)^{I}$	3.45(3)	97.8	$O(4')^{IV}$...O(6')	3.39(2)	98.3
O(4) ...O(7)	3.15(3)	90.8	$O(4')^{IV}$...$O(7')^{I}$	3.11(2)	88.8
O(4) ...$O(7')^{I}$	2.89(3)	81.1	$O(4')^{IV}$...O(7)	2.87(3)	79.7
O(4) ...W(2)	3.01(3)	86.1	$O(4')^{IV}$...W(2')	3.06(3)	87.5
O(3')...$O(6)^{I}$	2.78(2)	80.5	O(3) ...O(6')	2.81(2)	80.8
O(3')...O(7)	2.96(2)	87.4	O(3) ...$O(7')^{I}$	3.01(2)	88.6
O(3')...$O(7')^{I}$	2.86(2)	83.5	O(3) ...O(7)	2.92(2)	84.7
O(3')...W(2)	3.48(3)	109.2	O(3) ...W(2')	3.45(3)	108.0
O(6) ...$W(7')^{I}$	2.87(2)	83.2	O(6') ...O(7)	2.90(3)	83.6
O(6) ...W(2)	3.05(3)	90.1	O(6') ...W(2')	3.00(3)	88.8
O(7) ...$O(7')^{I}$	2.89(3)	84.2	$O(7')^{I}$...O(7)	2.89(3)	84.1
O(7) ...W(2)	3.39(3)	104.7	$O(7')^{I}$...W(2')	3.38(3)	105.4
Average	3.07		Average	3.07	

* Estimated standard deviations for distances are given in parentheses and refer to the last decimal place. The e.s.d.'s for the angles are 0.1°.

0.2783, slightly shifted from the correct position 1/4, 0, 1/4 of space group $P2_1/n$ (with the origin on the twofold screw axis). The coordinates of all pseudo-symmetric atoms obey the operation $0.5110 - x, \bar{y}, 0.5566 - z$ within 3σ, except for the pairs As(1),As(1') and As(2),As(2'), where deviations of 6σ and 10σ for x and for y, respectively, are observed. The ambiguous results of statistical tests on the intensities are accounted for by the pseudo-centrosymmetry of the structure; on the other hand the $h0l$ reflections with $h + l$ odd, which should be systematically absent if a true n plane were present, are only slightly weaker than the average: this is consistent with the pseudo-symmetry center being shifted from its proper position in space group $P2_1/n$.

The geometrical features of AsO_4 and MnO_6 coordination polyhedra are reported in Tables 2 and 3, respectively; pseudo-symmetry appears clearly in bond distances and angles. Polyhedra are connected by sharing edges and vertices and build up a system of (010) layers (Fig. 1); adjacent layers are related by the 2_1 operation and are linked by hydrogen bonding only (Fig. 2). Only translational symmetry is present within a single layer. The distorted coordination octahedra of Mn share edges with one another and form $[10\bar{1}]$ chains. The $O(2)^{II} \cdots O(2')$ and $O(3) \cdots O(6')$ edges are shared by the Mn(1) polyhedron with those of Mn(1') and Mn(2'), respectively; the Mn(2) and Mn(2') octahedra share the $O(7) \cdots O(7')^{I}$ edge, and the $O(3')^{IV} \cdots O(6)^{I}$ edge is

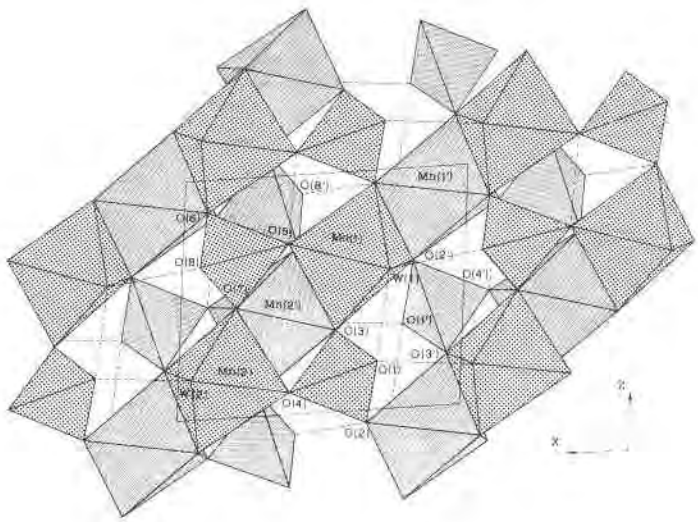

Fig. 1. Projection onto the plane (010) of one layer of the structure of krautite, emphasizing coordination polyhedra and intra-layer hydrogen bonds (dashed lines).

shared by the Mn(2) and Mn(1′) polyhedra. Chains are linked by the As tetrahedra, which share their O(2), O(3), O(4), O(2′), O(3′), O(4′) vertices with Mn octahedra. Chains belonging to adjacent layers are superposed exactly along y and are linked by inter-layer hydrogen bonds, building up (101) planes of chains; between them, planes are also formed by AsO_4 tetrahedra, which are connected by inter-layer hydrogen bonding as well.

The very strong mica-like {010} cleavage observed in the crystals of krautite is explained by the presence of weak hydrogen bonds between the (010) layers of coordination polyhedra. Two other cleavages are reported by Fontan *et al.* (1975): {101} and {$\bar{1}$01}. The former can be related structurally to the (101) alternate planes of Mn and As polyhedra, whereas the latter cannot be explained on crystal-chemical grounds, since it would involve the breaking of Mn octahedral chains which are the most strongly bonded in the structure.

Hydrogen bonding

Although the hydrogen atoms have not been located in the structure, no ambiguities are present in

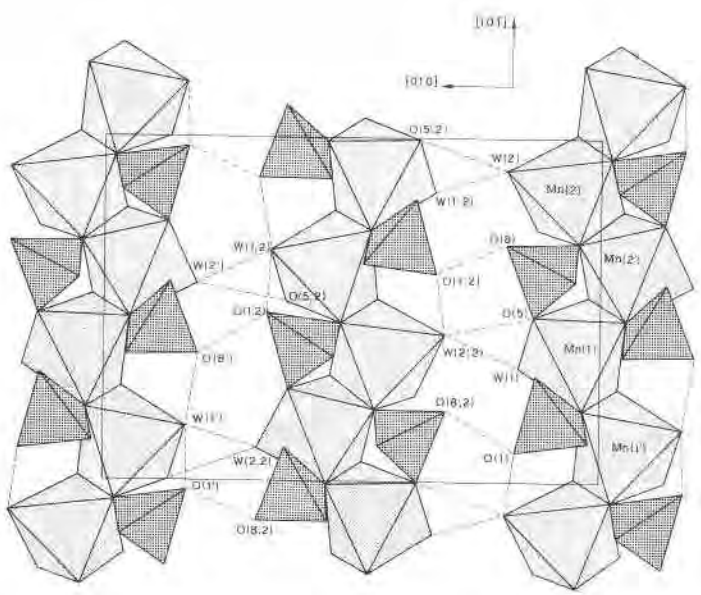

Fig. 2. Contents of one unit cell of krautite projected onto the (101) plane. Inter- and intra-layer hydrogen bonds are shown as dashed lines.

Table 4. Interatomic distances and angles in the hydrogen bonds

O(4) ...$O(5)^{I}$	2.58(2)* Å	As(1) - O(4) .. $O(5)^{I}$	112.5(8)°
O(4')...$O(5')^{III}$	2.61(2)	As(1') - O(4')..$O(5')^{III}$	112.3(7)
O(8) ...$O(1',2)^{VI}$	2.56(2)	As(2) - O(8) ..$O(1',2)^{VI}$	116.0(9)
O(8')...$O(1,2)^{V}$	2.60(2)	As(2') - O(8')..$O(1,2)^{V}$	115.4(9)
W(1) ...O(1)	2.64(2)	O(1) .. W(1)..$O(8)^{III}$	110.5(8)
W(1) ...$O(8)^{III}$	2.72(2)		
W(1')...$O(1')^{II}$	2.68(2)	$O(1')^{II}$.. W(1')..O(8')	108.4(7)
W(1')...O(8')	2.76(2)		
W(2) ...$O(1)^{IV}$	2.70(2)	$O(1)^{IV}$.. W(2)..$W(1',2)^{VI}$	130.2(8)
W(2) ...$W(1',2)^{VI}$	2.92(2)	$O(1)^{IV}$.. W(2)..$O(5',2)^{VII}$	73.4(6)
W(2) ...$O(5',2)^{VII}$	3.08(2)	$W(1',2)^{VI}$.. W(2)..$O(5',2)^{VII}$	58.9(5)
W(2')...O(1')	2.67(2)	O(1') .. W(2')..$W(1,2)^{V}$	128.8(8)
W(2')...$W(1,2)^{V}$	2.82(2)	O(1') .. W(2')..$O(5,2)^{V}$	71.3(6)
W(2')...$O(5,2)^{V}$	3.20(2)	$W(1,2)^{V}$.. W(2')..$O(5,2)^{V}$	58.5(5)

*Estimated standard deviations are given in parentheses and refer to the last decimal place.

the hydrogen bonding scheme (Table 4). On the basis of As–O bond lengths (Table 2), acidic hydrogen atoms can be unambiguously assigned to the oxygen atoms O(4), O(4′), O(8). The situation is less clear in the As(2′) tetrahedron, because the three longest As–O bonds are practically equal; however, only O(8′) is involved in a O ··· O contact, so the fourth acidic H atom has been assigned to it, in accordance with the pseudo-symmetry. The bonds donated by O(4) and O(4′) are contained in the (010) layers of coordination polyhedra, whereas those donated by O(8) and O(8′) link adjacent layers.

For the hydrogen bonds donated by water molecules, W(1) and W(1′) form four bonds connecting Mn octahedra to As tetrahedra inside the (010) layer; W(1) ··· O(1) and W(1′) ··· $O(1')^{II}$ are very short and thus strong bonds, while the other two lie in the range of medium-strength bonds. Two medium-strong intra-layer bonds are donated by W(2) and W(2′) to $O(1)^{IV}$ and O(1′), respectively. W(2) shows two additional rather long interlayer contacts with $W(1',2)^{VI}$ and $O(5',2)^{VII}$, which could reasonably form a bifurcated hydrogen bond, taking into account the values of the three angles $O(1)^{IV}$ ··· W(2) ··· $W(1',2)^{VI}$,$O(1)^{IV}$ ··· W(2) ··· $O(5',2)^{VII}$ and $W(1',2)^{VI}$ ··· W(2) ··· $O(5',2)^{VII}$. The two pseudosymmetric contacts of W(2′) with $W(1,2)^{V}$ and $O(5,2)^{V}$ have different lengths, with the second contact at about the distance limit for a significant interaction; we conclude that the existence of a bifurcated hydrogen bond is less likely for W(2′) than for W(2).

Table 5. Bond valences and their sums (Σ) for each atom, calculated by Brown's (1976) curve for hydrogen bonds and by Brown and Wu's (1976) universal formula for other bonds

	As(1)	As(1')	As(2)	As(2')	Mn(1)	Mn(1')	Mn(2)	Mn(2')	O(1)	O(1')	O(4)	O(4')	O(5)	O(5')	O(8)	O(8')	W(1)	W(1')	W(2)	W(2')	Σ
O(1)	1.31															0.30	0.26		0.22		2.09
O(1')		1.46													0.34			0.24		0.24	2.28
O(2)	1.41				0.36	0.32															2.09
O(2')		1.22			0.34	0.37															1.93
O(3)	1.31				0.32			0.36													1.99
O(3')		1.22				0.31	0.39														1.92
O(4)	0.92						0.27						0.70								1.89
O(4')		1.06						0.25						0.71							2.02
O(5)			1.26		0.26						0.30									0.05	1.88
O(5')				1.36		0.29						0.29							0.08		2.02
O(6)			1.26			0.36	0.35														1.97
O(6')				1.18	0.37			0.35													1.90
O(7)			1.26				0.37	0.34													1.97
O(7')				1.22			0.36	0.38													1.96
O(8)			1.06							0.66							0.20				1.92
O(8')				1.22					0.70									0.19			2.12
W(1)					0.31				0.74						0.80					0.15	2.00
W(1')						0.29				0.76				0.40		0.82			0.11		1.99
W(2)							0.39		0.78									0.41			1.98
W(2')								0.41					0.30							0.50	1.97
Σ	4.95	4.96	4.84	4.98	1.96	1.94	2.13	2.09													

The consistency of this hydrogen bonding scheme can be tested in two ways: (i) by comparing the experimental bond lengths with those predicted by Baur's (1970) empirical correlations with the bond strengths (Pauling's second rule); (ii) by calculating bond valences based upon experimental bond lengths (Brown and Wu, 1976; Brown, 1976), and checking that the sums on each atom fit its theoretical valence. Both approaches have given satisfactory results, taking into account the low accuracy of bond distances; bond valence values are reported in Table 5.

Crystal-chemical comparison with haidingerite and pharmacolite

The structures of haidingerite, $CaHAsO_4 \cdot H_2O$ (Cassien *et al.*, 1966; Calleri and Ferraris, 1967), and pharmacolite, $CaHAsO_4 \cdot 2H_2O$ (Ferraris, 1969), are closely related to that of krautite: all these minerals are built up of (010) layers of coordination polyhedra held together by hydrogen bonding. This similarity is reflected in the unit-cell parameters, which are reported in Table 6; data for haidingerite are taken from Calleri and Ferraris (1967), but *a* and *c* have been interchanged. For pharmacolite, the primitive unit cell reported by Ferraris (1969) is not suitable for this comparison, since only four unit-formulas are contained instead of eight; by applying the transformation $10\bar{1}/010/101$ to it, the double cell shown in Table 6 is obtained.

Differences between the three structures appear in the single-layer topology of the coordination polyhedra, and are due to two causes: (i) different cation coordination number in krautite (Mn^{2+}, CN = 6) with respect to haidingerite and pharmacolite (Ca^{2+}, CN = 7); (ii) different water content in pharmacolite ($2H_2O$) with respect to krautite and haidingerite ($1H_2O$). Haidingerite is characterized by low hydration and high cation coordination number. The CaO_7 polyhedra share several edges and vertices and show a very condensed configuration, forming a two-dimensional framework. On the other hand, the topology of the pharmacolite layer is very similar to that of krautite, since high hydration and high CN of the cation balance each other; the CaO_7 polyhedra share edges and build up $[10\bar{1}]$ chains which sandwich the AsO_4 tetrahedra. The (010) layers are stacked in a different way from krautite; they are related by a glide plane, so that chains of adjacent layers are staggered instead of being superposed as in the latter mineral.

Krautite structurally resembles the dihydrated phase of calcium hydrogen arsenate more than the monohydrated phase, for the same reasons that the structure of LiH_2PO_4 is closer to $NaH_2PO_4 \cdot H_2O$ than to NaH_2PO_4: "the same effect is produced by either lowering the coordination number of the cation or introducing water molecules into the crystal lattice: the ratio of the number of available oxygen atoms to the number of vertices of the cation polyhedron increases, so that decondensation of cation polyhedra occurs" (Catti and Ivaldi, 1977).

Table 6. Unit-cell data of krautite and related minerals

	Krautite	Haidingerite	Pharmacolite*
S.G.	$P2_1$	Pbna	Fn
a	8.012	7.935	10.327 Å
b	15.956	16.161	15.434
c	6.801	6.904	6.604
β	96.60		93.15°
V	863.7	885.4	1051.0 Å^3
Z	8	8	8
Chemical formula	$MnHAsO_4 \cdot H_2O$	$CaHAsO_4 \cdot H_2O$	$CaHAsO_4 \cdot 2H_2O$

* Double cell.

Acknowledgments

We thank Professor F. Permingeat (University of Toulouse, France) for sending us the manuscript of his paper on the new mineral $CaMn(HAsO_4)_2 \cdot 2H_2O$, in preparation. The X-ray intensities were measured at the Centro di Studio del C.N.R. per la Cristallografia Strutturale, Pavia. The research was supported by the Consiglio Nazionale delle Ricerche, Roma.

References

Baur, W. H. (1970) Bond length variation and distorted coordination polyhedra in inorganic crystals. *Trans. Am. Crystallogr. Assoc., 6,* 129–155.

Brown, I. D. (1976) On the geometry of O–H ··· O hydrogen bonds. *Acta Crystallogr., A32,* 24–31.

——— and K. K. Wu (1976) Empirical parameters for calculating cation–oxygen bond valences. *Acta Crystallogr., B32,* 1957–1959.

Calleri, M. and G. Ferraris (1967) Struttura della haidingerite: $CaH(AsO_4) \cdot H_2O$. *Periodico Mineral., 36,* 1–23.

Cassien, M., P. Herpin and F. Permingeat (1966) Structure cristalline de la haidingérite. *Bull. Soc. fr. Minéral. Cristallogr., 89,* 18–22.

Catti, M. and G. Ivaldi (1977) Crystal structure of LiH_2PO_4, structural topology and hydrogen bonding in the alkaline dihydrogen orthophosphates. *Z. Kristallogr., 146,* 215–226.

———, G. Ferraris and G. Ivaldi (1977) Hydrogen bonding in the crystalline state. Structure of talmessite, $Ca_2(Mg,Co)(AsO_4)_2 \cdot 2H_2O$, and crystal chemistry of related minerals. *Bull. Soc. fr. Minéral. Cristallogr., 100,* 230–236.

Deiss, E. (1914) Ueber Herstellung und Eigenschaften der Manganoarsenatgallerte. *Kolloid Z., 14,* 139–146.

Ferraris, G. (1969) The crystal structure of pharmacolite, $CaH(AsO_4) \cdot 2H_2O$. *Acta Crystallogr., B25,* 1544–1550.

Fontan, F., M. Orliac and F. Permingeat (1975) La krautite $MnHAsO_4 \cdot H_2O$, une nouvelle espèce minérale. *Bull. Soc. fr. Minéral. Cristallogr., 98,* 78–84.

Germain, G., P. Main and M. M. Woolfson (1971) The application of phase relationships to complex structures III. The optimum use of phase relationships. *Acta Crystallogr., A27,* 368–376.

Moore, P. B. (1967) Contributions to Swedish mineralogy: I. Studies on the basic arsenates of manganese. *Ark. Mineral. Geol., Stockholm, 4,* 425–444.

Pascal, P. (1966) *Nouveau Traité de Chimie Minérale, Vol. XVI.* Masson, Paris.

Protas, J. and R. Gindt (1976) Structure cristalline de la brassite, $MgHAsO_4 \cdot 4H_2O$, produit de désydratation de la roesslérite. *Acta Crystallogr., B32,* 1460–1466.

Manuscript received, January 2, 1979;
accepted for publication, July 9, 1979.